Prediction of Time of Death Using a Heat Transport Model

Jimmy L. Smart, PhD[1*], Michal Kaliszan, MD, PhD[2]

[1]University of Kentucky, Paducah, KY, USA, [2]Medical University of Gdansk, Poland

*Corresponding author: 4810 Alben Barkley Drive, Paducah, KY 42001, jsmart@engr.uky.edu

Abstract: COMSOL Multiphysics® 4.0 was used to study conductive and convective heat transfer from the human eyeball to the surrounding air. A postmortem temperature decay curve was collected from an eyeball of a recently deceased human body. Of course, this curve represents only a portion of the complete temperature decay curve, since there is a time lapse between when an individual has died and when the pathologist is able to start collecting temperature data. This portions of the actual cooling curve was compared to a complete model cooling curve developed with COMSOL finite element method software. Theoretically, if a model cooling curve can be superimposed exactly upon the actual cooling curve, time of death can be reliably predicted. The model fitted the experimental data with an R^2 = 0.987. Various reasons are offered to explain deviations between the COMSOL model and the actual temperature decay curves.

Keywords: time of death, heat transfer, heat conduction, finite element model, heat transport in human eye.

1. Introduction

Most "time of death" predictive models for humans have been based upon torso modeling and rectal temperature profiles [1,2]. This approach has not been entirely satisfactory, and to date, time of death approximations are not admissible into a court of law. A number of factors can explain the problem, including significant variability in tissue size and distribution across human bodies in the general population. All human torso morphologies are different, so a single reproducible a priori "one size fits all" model is not practical. A more reliable approach to estimating postmortem temperature decay is believed to be based upon the human eyeball. Eye structure, skull, and brain are relatively consistent across human populations. Actual head size, which includes fluids/adipose tissue will vary, and is equal to 7.3% of the overall body weight [3]. This study will focus upon temperature decay within the human eyeball.

2. Postmortem Temperature Decay Curves

Experimental postmortem temperature decay measurements were conducted on individuals who died of sudden death, with known exact time of death. The bodies were transferred to the Department of Forensic Medicine, Medical University of Gdańsk, Poland for autopsy. The study was performed according to the regulations of the ethics committee for studies on humans at the Medical University of Gdańsk (individual approval no. NKEBN/144/2010).

Experimental temperature recordings were collected at room temperature. Measurements were performed using P655 two-channel thermometers connected to 1 mm wide pin probes (Dostmann–electronic GmbH, Wertheim-Reicholzheim, Germany). During temperature recording, the human bodies were resting face-up on 1 meter high metal wheel carts, isolated from the environment.

After attaching an eyelid spreader to obtain a wide eyelid slit, the eyeballs were stabilized with stabilizing forceps. Pin probes were inserted into the sclera of the nasal quadrants of the eyeballs, 3-mm away from the corneal limbus, passing through the pars plana of the ciliary body into the vitreous chamber, and then further on, posterior and laterally from the optic nerve head, at a depth of 22 mm. Another pin probe was inserted into the soft tissues of the orbits at the median canthus, passing along the medial rectus

muscle towards the superior orbital fissure, at a depth of 25 mm.

The probes used in each set of measurements were stabilized within the grips of stands. When the probes had been stabilized, special care was taken to ensure that they did not cause the eyelids to be open (the eyelids were naturally closed in all the studied bodies).

The ambient temperature was measured using a probe placed 1 meter above the floor in the central part of the room. All thermometers were connected to a computer programmed to record the temperature values every 5 minutes. The procedure preceding starting the recording device lasted up to 3 hr post mortem. The recording of measurements was completed after around 15 hours post mortem.

3. Finite Element Model

3.1 Heat Transport Theory

Once a human expires, a temperature gradient within the body is established, and a normal body temperature of approximately 37 ^{o}C begins to decay. The rate of decay is influenced by a variety of factors, including surrounding air temperature, convection conditions, and tissue composition/ geometry [2]. Postmortem temperature decay within the body is basically a study of unsteady state heat conduction, driven by external natural convection. Convective effects at the interface of the skin and surroundings provide the driving force for heat to be transported from the warmer eyeball through surrounding tissues into the cooler environment. This study deals only with natural convection, but the model could be easily modified to include various conditions of forced convection provided by a fan, an air conditioner, or wind blowing across the face.

Over time, as the eye loses heat to the surrounding environment, a temperature decay curve is traced. If this actual unique curve could be successfully modeled, a crime scene investigator could use this information to estimate time of death.

3.2 Governing Equations

The classical equation used to describe heat conduction is [4]:

$$\rho C_p \frac{\partial T}{\partial t} - \nabla \cdot (k \nabla T) = Q \qquad eq\ (1)$$

COMSOL software offers several choices for equations to accommodate conditions of natural convection, including convection from a vertical plate and convection from a horizontal plate (face up or face down). Also, equations within the software can be modified to describe other geometries. Since the human head is approximately spherical, an empirical relationship for natural convection from a sphere [4] was a rational choice:

$$\frac{hD}{k} = 2 + \frac{0.589\, Ra_D^{1/4}}{\left[1+\left(\frac{0.469}{\mathrm{Pr}}\right)^{9/16}\right]^{4/9}} \qquad eq\ (2)$$

3.3 Model Construction

In this study, a 3D model of the human head containing both detailed eyeball geometries, brain, skull, brain bone casing, eyeball bone casing, and major head sinuses was constructed.

First, detailed eye geometry was patterned after Ng et al. [5]. These investigators constructed a 2D finite element model to evaluate temperature distributions within the human eye. Half plane geometry of the assembled 2D eye is shown in Figure 1.

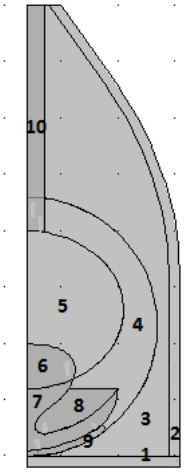

Fig. 1 Half Plane of 2D Eye Morphology
1. Eyelid
2. Bone housing

3. Orbit fat/muscle/fluid
4. Sclera
5. Vitreous humor
6. Lens
7. Aqueous humor
8. Iris
9. Cornea
10. Optic nerve

Next, to form the 3D geometry, the 2D geometry shown in Figure 1 was revolved 360°. The final 3D eye geometry for both eyes is shown in Figure 2. Figure 3 shows the 3D geometry of the eye with some structures removed to aid in visualization; the left eye has the bone housing and the orbit fat/fluid removed, and the right eye has the additional sclera removed.

Even though geometries and local tissue distributions of the human eye are relatively consistent across human populations, there is still variability across head size, sinuses, skin, skull, etc. Detailed anatomy of the human eye and head is very complex. Great care was exercised in preparation of the 3D model of the human eye, but inclusion of more detailed morphologies within the head (blood vessels, musculature, nerves, spine, etc.) were not justified, as these additions did not significantly affect temperature decay profiles.

Fig. 2 360° Revolution of Half Plane Eye Morphology.

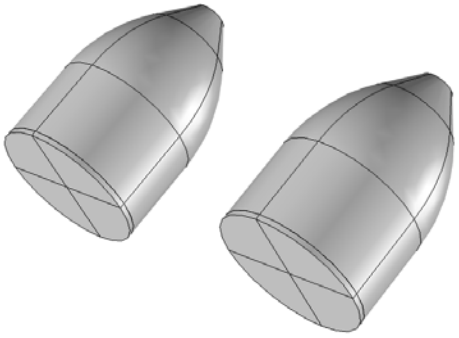

Fig. 3 3D Eye Model with Some Structures Missing to Aid in Visualization.

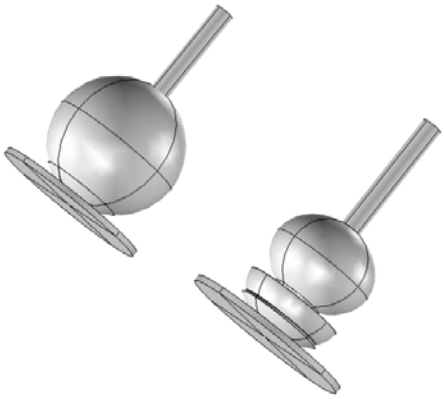

Using anatomical imaging from Bo et al. [6], major morphologies within the 3D head model were inserted, including skull, sinuses, brain, brain bone casing, and eyeball bone casing. The rest of the head tissues were lumped together and assigned one set of thermal properties. Figure 4 is the final 3D model of the head and Figure 5 is a transparent view of the final 3D head model. Thermal properties of various tissues are summarized in Table I.

Major sinuses (ethmoid, frontal, and maxillary) and nasal passageways were incorporated into the model.

Fig. 4 Final 3D Model of the Head Including Eyeballs and Surrounding Morphologies.

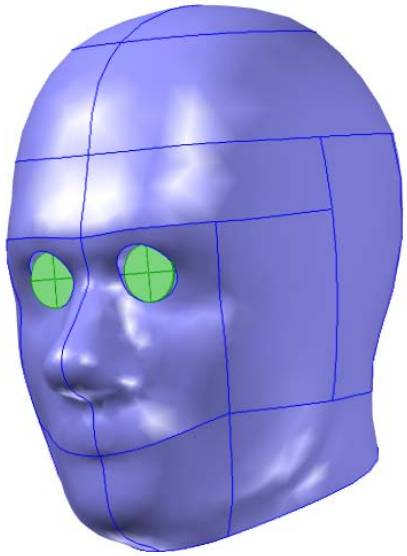

Initial temperatures within the eye include the cornea at 34.3 °C and the mean temperature

of the eye at 36.0 ^{o}C [5]. Initial temperature of the skin, including the eyelid temperature was set at 35.0 ^{o}C. Initial core temperature, including the head, brain, bone housings of the eyes and the brain were set at 37 ^{o}C. Surrounding air temperature was set for conditions experienced within the morgue, where temperature decay was measured, generally 20 – 22 ^{o}C.

3.4 Model Execution

Using a Dell Optiplex® 760 (Intel Core Duo E8400, 3 GHz processor, 8 GB RAM, 64 bit), and depending upon the selected mesh size, the model takes about 3.5 – 17.5 minutes to execute.

Meshing size from extra coarse to extra fine did not have any significant effect upon the final temperature decay model curve.

4. Results

4.1 Effect of Convective Coefficient

Using a characteristic diameter of 0.22 m, the empirical equation for the convective heat transfer coefficient for a sphere, shown previously as eq (2), was applied with unsatisfactory results, i.e., convective heat transfer coefficient was underestimated. A value of 55 was substituted in place of the lead coefficient value of 2 in eq (2) with improved results. See Figure 6.

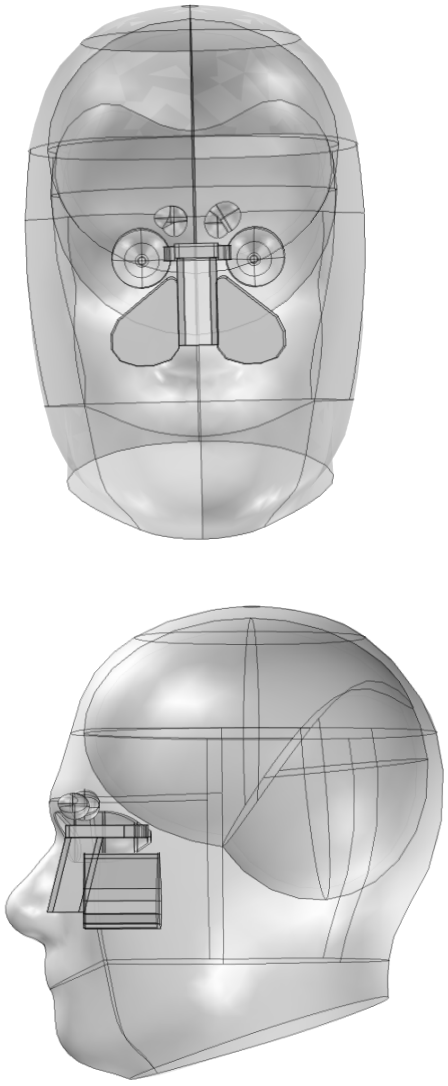

Fig. 5 Front and Side Transparent Profile Views of the 3D Model of the Head, Including Eyeballs and Surrounding Morphologies.

Table 1: Thermal Properties of Human Tissue

	k	C_p	ρ
cornea [5]	0.58	4178	1050
aqueous humor [5]	0.58	3997	996
iris [5]	1.0042	3180	1100
lens [5]	0.40	3000	1050
vitreous body [5]	0.603	4178	1000
sclera [5]	1.0042	3180	1100
Eye fat/ fluid [7]	0.21	2300	920
bone [7]	0.75	1700	1357
brain [7]	0.49	3850	1080
skin [7]	0.47	3680	1085

Using eq (2) with a lead coefficient of 55, the convective heat transfer coefficient within the model at the highest driving force was 7.9 W/m^2 hr K, and varied to a low value of 6.1 W/m^2 hr K at the lowest driving force. Scott [8] used a fixed value of 10 W/m^2 K for the convective coefficient in her finite element model of the human eye. Ng et al. [5] used values of 8, 10, 15 and 100 W/m^2 K in their sensitivity analysis to evaluate how sensitive were changes in temperatures across the 2D eye to changes in the convective heat transfer coefficient. As shown in Figure 6, use of constant values of convective heat transfer coefficients of 6 and 10 within the model did not provide a satisfactory fit.

Fig. 6 Effect of Convective Heat Transfer Coefficient Upon Model Results.

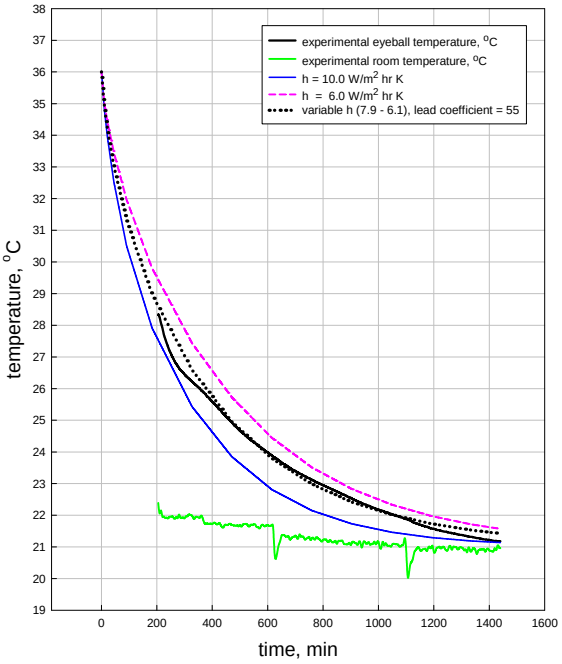

4.2 Sensitivity Analysis

Temperature profiles at specific points across the diameter of the eyeball did not significantly vary over time. For example, using an average convective coefficient of 10.0 W/m^2 hr K, after 10 hrs, temperatures at the cornea, middle of the vitreous humor, and inside sclera wall were 22.6, 22.9, and 23.2 ^{o}C respectively.

5. Discussion

As previously pointed out, the empirical relationship, eq (2), for convective heat transfer from a sphere could not be reliably used when modeling the human head. Besides the idea that the head is only approximately spherical, this is probably due to additional turbulent effects caused by nose and other structures on the surface of the head. Also, the neck transports heat by conduction, rather than by convection. Therefore, to modify eq (2) to better describe natural convective heat transfer from the human head, the lead coefficient in eq (2) was changed from 2 to 55.

Theoretically, if a model cooling curve can be superimposed exactly upon the actual cooling curve, time of death can be reliably predicted. Based upon the results shown in Figure 6, the model fitted the experimental data with a coefficient of determination, $R^2 = 0.987$.

Further refinements of the model will hopefully improve its predictive quality. These refinements will include:

(a) Incorporation of additional experimental data.

(b) The current model assumes a fixed temperature of the surrounding air. A future improvement of the model will incorporate an analytic function to describe the variation of the temperature of the surrounding air.

(c) A cursory view of additional experimental data (data not shown or evaluated in this present study) shows variation of head mass from 5.3 – 7.6 kg. An improved COMSOL model allow for variations in head mass.

(d) There is a phenomenon called the "temperature plateau" effect, whereby there is a delay between the time of death and when a temperature gradient is established, leading to the point when the body commences to cool. When measuring rectal temperatures, this plateau can be as long as 5 – 6 hours [7]. Since the eyeball is a smaller structure and is surrounded by less tissue, the temperature plateau period is reduced. This temperature plateau effect will also

be included in future improvements of the COMSOL model.

6. Conclusions

Due to the relative consistency of eyeball and head morphologies across various human populations, it was believed that using a heat transport model of the human eye would serve as a reliable model for predicting time of death. As evaluated from a sensitivity study in a previous study [2], temperature decay models are very sensitive to the initial temperature of the body (eyeball/head) and temperature of the surrounding environment.

Additional postmortem experimental data is being collected to allow further refinement of the COMSOL computer model. Also, forced convection effects will be studied.

7. References

1. Henssge, Claus, *The Estimation of the Time Since Death in the Early Postmortem Period*, 2nd ed., London: Arnold Publishing (2002).
2. Smart, Jimmy L, Estimation of Time of Death With a Fourier Series Unsteady State Heat Transfer Model, *J. Forensic Sci*., 1-7 (June 2010).
3. Clauser, C.E., J.T. McConville, and J.T. Young, Weight, Volume, and Center of Mass Segments of the Human Body, *Wright-Patterson Air Force Base, Ohio: US Air Force, AMRL-TR-69-70* (1969).
4. Incropera, F.P. and D.P. Witt, *Fundamentals of Heat and Mass Transfer*, 4th ed. John Wiley & Sons (1996).
5. Ng, E.Y.K. and E.H. Ooi, FEM Simulation of the Eye Structure with Bioheat Analysis, *Computer Methods and Programs in Biomedicine*, **82**, 268-276 (2006).
6. Bo, WJ, NT Wolfman, WAK Krueger, and I Meschan, *Basic Atlas of Sectional Anatomy with Correlated Imaging*, Philadelphia: W.B. Saunders Co (1990).
7. Mall, G and W Eisenmenger, Estimation of Time Since Death by Heat-Flow Finite-Element Model. Part I: Method, Model, Calibration, and Validation, *Legal Med*., **7**, 1- 14 (2005).
8. Scott, J.A., A Finite Element Model of Heat Transport in the Human Eye, *Phys. Med. Biol.*, **33(2),** 227-241 (1988).
9. Kaliszan, M, R Hauser, J Buczynski, et al., The Potential Use of the Eye Temperature Decrease in Determining the Time of Death in the Early Postmortem Period, *Am. Forensic Med. Pathol.*, **31(2**), 162-164 (June 2010).

8. Acknowledgements

Dr.Kaliszan would like to thank Dr. Zbigniew Jankowski for help in arrangement and collection of post mortem temperature decay data.

COMSOL support staff provided the exterior head geometry for the 3D model.

9. Nomenclature

Cp	heat capacity, J/kg K
D	diameter, m
h	heat transfer coefficient, W/ m^2 K
k	thermal conductivity, W/m K
Pr	Prandtl number, dimensionless
Ra_D	Rayleigh number, dimensionless
ρ	density, kg/m^3
T	temperature, K
T_{inf}	initial temperature of the eye, K
T_{amb}	ambient surrounding temperature, K
t	time, s